IEEE Access
Multidisciplinary | Rapid Review | Open Access Journal

Received June 11, 2021, accepted June 28, 2021, date of publication July 12, 2021, date of current version July 21, 2021.

Digital Object Identifier 10.1109/ACCESS.2021.3096649

Remote Professional Media Production: Evaluation of Network Configuration That Satisfies Delay Requirements

JUNICHIRO KAWAMOTO, RYO SHIRATO, TSUYOSHI NAKATOGAWA, (Member, IEEE), AND TAKUYA KURAKAKE

Science and Technology Research Laboratories, Japan Broadcasting Corporation (NHK), Tokyo 157-8510, Japan

Corresponding author: Junichiro Kawamoto (kawamoto.j-he@nhk.or.jp)

ABSTRACT With the shift to the Internet Protocol (IP) in professional media production, the demand for a remote professional media production system (hereinafter ''remote production'') is increasing. In remote production, a venue is connected with a broadcasting station by an IP network, and live programs are produced not on the venue side but on the broadcasting station side. In recent years, flexible remote production systems that use cloud computing over the IP network have been considered. In this work, to achieve remote production using a low-latency cloud, we examined the roundtrip-delay requirement for remote production and investigated which network configurations satisfied this requirement by testing network models from Japan, Europe, the USA, and China, which included metropolitan area networks. Two different program production equipment configurations were examined: a diverse path configuration with seamless switching (DPC) and a single path configuration with forward error correction processing (SPC). The results showed that the roundtrip-delay requirement was 33.4 ms (one-way transmission-delay: 16.7 ms) and that the server processing latency in the cloud should be kept in the range of 2–6 ms to satisfy the transmission-delay requirement for achieving a coverage rate of approximately 50% when using DPC and SPC for program production equipment configurations. We also found that, in all network models, SPC was better able to improve the coverage rate while satisfying the transmission-delay requirement than DPC. These findings should be useful for helping broadcasters design remote production systems using a low-latency cloud network.

INDEX TERMS IP network, metropolitan area networks, remote production.

I. INTRODUCTION

In recent years, due to an increase in communication speed and a decrease in bit costs, a flexible and efficient network with Internet Protocol (IP) technology has spread worldwide. The field of broadcasting technology is not an exception. Standardization of IP-based signal transmission technologies as specified in the Society of Motion Picture and Television Engineers (SMPTE) ST 2110 suite has been performed, and the introduction of professional media production facilities is in progress [1]–[3].

Serial digital interfaces (SDIs) have been used for many years in the program production field of professional media broadcasting stations as a basic transmission signal that can consistently achieve high-quality and stable broadcasting services. SDI is a unicast and unidirectional transmission signal that transmits one type of signal on one coaxial cable [4]. In contrast, IP technology is characterized by unicast/multicast signals, bidirectionality, and ease of multiplexing. In recent years, a 400-Gb/s Ethernet transmission standard [5] has been completed, leading to a speedup, and the consequent commoditization of devices is also remarkable. Thus, IP has a high affinity for enabling a wide variety of broadcasting services. Furthermore, the introduction of IP not only improves transmission efficiency but also has the potential to provide new workflows in program production system operations, such as collaboration with the software and the cloud [6]–[9]. IP has particularly been attracting attention in remote production, where a venue is connected with a broadcasting station by the IP network and live programs are produced not on the venue side but rather on the broadcasting station side [10]. The introduction of this

The associate editor coordinating the review of this manuscript and approving it for publication was Jon Montalban.

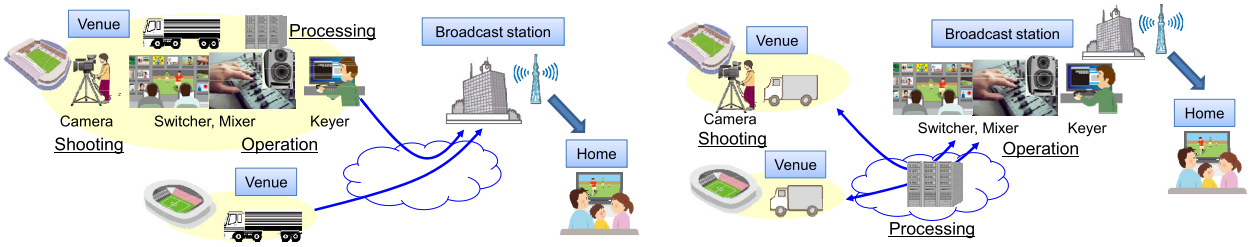

(a) Conventional production work style

(b) Remote production work style

FIGURE 1. Overview of conventional production work style and remote production work style. The most significant difference between these work styles is whether the program production is done at the venue or from the remote broadcast station.

production technique is expected to bring various benefits, such as improved availability of the broadcasting equipment installed on the broadcasting station side and the realization of flexible working styles for the producer.

Fig. 1(a) shows a conventional production work style, and Fig. 1(b) shows a remote production work style. In the conventional production work style, a large outside broadcasting (OB) van is typically placed at each venue, and production work (e.g., switching between field camera videos, mixing audio) is carried out in the van using broadcasting equipment connected by SDI signals. The resulting signals are compressed to tens or even to 1/100 of the original size and then broadcast from a broadcasting station to customer homes. Because shooting, operation and processing are basically completed at the venue, the transmission delay of the SDI signal from the field camera to the video switcher is very small. Especially in cases such as live sports production, the camera operator needs to immediately control the camera while comparing the video being shot by the camera with the video after switching or other operations have been performed. Also, when using a wipe effect to the live video, the camera operator needs to control the camera while watching the real-time video after switching in order to make perfect composition adjustments. For these reasons, it is desirable that the delay between the field camera and the video switcher be small. On the other hand, in the remote production work style, the operation is typically carried out from the broadcast station to various remote places, and in some cases, the processing is performed in the cloud. In such cases, the transmission delay composing a roundtrip delay becomes a problem due to the distance between the venue and the broadcast station. This delay is mainly the combination of the processing delay of the program transmission equipment for performing remote production and the network delay that the signal propagates through the network, and it occurs in both directions between the venue and the broadcasting station [11].

In light of the above, the following two points should be addressed in remote production: (1) what is the roundtrip-delay requirement that would enable the same operation as the conventional production work style, even at the time of remote production (e.g., ensuring that the roundtrip delay between a shot video and a return video after switching is small); and (2) whether the aforementioned roundtrip-delay requirement can be met when the assumed network configuration using the cloud and quality compensation technology applied in a network model in consideration of geographical factors and how to set the server processing latency in the cloud. Therefore, in this paper, we first test the roundtrip-delay requirement based on an actual remote production system and then, on the basis of the results, evaluate which network configuration can enable remote production on a model similar to the actual network of major telecommunications carriers in Japan, Europe, the USA, and China. Section 2 of this paper refers to the state of the art related to research on transmission delays. Section 3 summarizes the requirements for the remote production network configuration. Section 4 clarifies the roundtrip-delay requirement during remote production. Section 5 examines the network configuration based on the obtained roundtrip-delay criterion and evaluates the area coverage of remote production that can meet the roundtrip-delay requirement.

II. STATE OF THE ART

The end-to-end delay requirement has been studied in various application fields. For example, in virtual reality (VR), the delay needs to be less than 20 ms, and 60 ms is usually taken as an upper bound for an acceptable VR experience [12], [13]. Additionally, for robotics and telepresence, a delay of a few milliseconds is desired, and a delay as low as 1 ms is desired for a tactile Internet experience using a mobile edge cloud [14]–[18]. As the end-to-end delay requirements have not been defined for the remote production of professional media, the topic we tackle in the current work has a high value.

In a previous work, with the objective of reducing the processing delay of program transmission equipment in remote production, we developed a lightweight compressed 8K IP transmission device that can transmit 8K videos with high image quality and a low delay [19]. In this system, the program transmission device compresses 8K videos to 1/5–1/9 and can transmit and receive with a processing delay of 1 ms or less. Since the transmission bandwidth of uncompressed 8K is over 40 Gb/s, it is necessary to consider compressed transmission that achieves transmission efficiency with low delay, such as JPEG XS [20].

Although prior studies on network delays have been conducted [21], [22], they focused on transmission delays in one direction, and no studies have adequately examined the delay requirements related to remote production. Therefore, we need to clarify how much transmission delay (roundtrip delay) is permissible for remote production and, in other words, how much transmission delay is required to enable program production similar to the conventional production work style.

Furthermore, the processing delay and the network delay constituting the transmission delay vary depending on the configuration of the program transmission equipment and the network. For high-quality and stable program production, we need to consider the transmission delay in terms of both the network configuration (e.g., diverse paths or single path, processing latency of switches, routers, and computing servers in the cloud) and the quality compensation technology (e.g., seamless switching or forward error correction -FEC-processing) in a real propagation environment. To consider the transmission delay, we can determine whether the configurations of the program transmission equipment and the network used between the venue and the broadcast station meet the transmission delay requirements for remote production at the planning stage before remote production is performed. Thus far, Kawamoto *et al.* [23] examined a case in which a diverse path network configuration was used, but there has been no discussion on quality compensation technology. The evaluation of delay by modeling networks has been done in the past. For example, in Petrov *et al.* [24], the end-to-end (E2E) packet delay of best-effort traffic due to the increase in mission-critical traffic was evaluated in softwarized 5G networks. Additionally, in Ye *et al.* [25], the average E2E delay was analytically derived as a variable D_i in 5G core networks with an embedded virtual network function chain. Modeling considering traffic patterns in real applications [26] and delay prediction in cut-through switching networks has also been examined [27]. Regarding latency in the cloud, some studies have reported how to achieve a processing latency of a few milliseconds [28]–[31]. However, no consideration has been given to cloud network configurations satisfying delay requirements that take redundancy and error correction into account. In the conventional production work style, it has been possible to produce high-quality and stable programs with almost no signal errors because the program production is done at the venue. On the other hand, in remote production, because program production is performed over networks, it is necessary to consider network redundancy and error correction to compensate for errors caused by network equipment failures or degradation of transmission channel quality. This novel approach is considered in this paper.

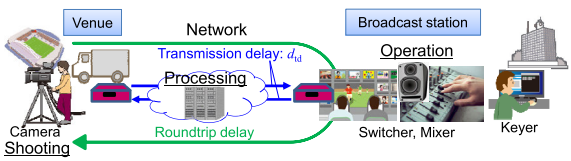

FIGURE 2. Overview of remote production. Program production over a network from a remote location enables efficient program production. However, the delay caused by the distance affects the production quality.

III. REQUIREMENTS FOR NETWORK CONFIGURATION

Fig. 2 shows an overview of remote production using the cloud. With remote production using the cloud, the venue and the broadcasting station are connected by an IP network, and the program production operations are carried out not at the venue but rather at the broadcasting station, while the program production processing (e.g., video effects, audio mixing) is carried out in the cloud. Since remote production is essentially performed between remote places, a delay caused by the distance always occurs. To achieve optimal remote production, it is necessary to transmit high-quality video from the venue to the broadcasting station with a small delay and to transmit the return video switched at the broadcasting station to the venue with a small delay. In short, to achieve operation with little sense of incongruity that is on par with the conventional production work style in remote production using the cloud, it is important to grasp this round-trip delay. We refer to this as the roundtrip-delay requirement in this paper.

The two network configuration requirements for remote production are as follows:

i. To satisfy the roundtrip-delay requirement in a delay time difference between video shot at the venue and the video returned from the broadcasting station.
ii. To provide a network and program transmission equipment configuration that can perform the high-quality video transmission required in program production.

Regarding the first requirement, although the production signals include audio signals and control signals in addition to video signals, it is more important to consider the delay caused by the transmission of video signals when producing a program. If the delay is larger than necessary, it becomes difficult to express the direction intended by the producer. In particular, in bidirectional video transmission over the network, the delay of the video signal has a significant effect [32]. Therefore, to meet this requirement, we need to consider the delay time difference between the shot video at the venue and the return video from the broadcasting station and grasp how much delay is acceptable compared to the delay with the conventional production work style using SDI.

In the case of transmission over the network, noise may occur in the video to be reproduced due to deterioration of transmission quality caused by transmission packet jitter, congestion, loss, and so on. As described in the second requirement, since high-quality video production is required in the program production of a broadcasting station, measures for continuing stable broadcasting even when transmission quality deteriorates are desired in both networks and transmission devices. In the case of a configuration capable of duplicating the network to be transmitted, two separate paths are prepared as a main system and a standby

system, and when the transmission quality of the main system deteriorates, the signals are switched to the standby system. To switch the video while not generating noise, a buffer for absorbing the delay time difference between the two paths at the receiver side and for switching seamlessly [33] is required in section 6.2, SMPTE ST 2110–10 [1]. We refer to this configuration as the diverse path configuration with seamless switching.

In the case of a configuration for transmission by the single path network, to realize high-quality video transmission even when error occurs, a quality deterioration compensation technique is desired for the transmitter and receiver. Representative quality degradation compensation techniques include retransmission control and FEC. In retransmission control, when the transmission quality deteriorates, the receiver side requests the transmitter side to retransmit the packet whose quality deteriorates, and the transmitter side retransmits the packet. This method increases the delay. In contrast, FEC is generally a technique in which a redundant signal is transmitted simultaneously with the transmission of a video signal on the transmitter side, and when quality deterioration is detected on the receiver side, the redundant signal is used to compensate for the quality deterioration. In the case of the configuration using FEC, since redundant signals are always transmitted, the transmission band is increased, but quality compensation becomes possible with delay related to the encoding and decoding of FEC. In other words, since FEC enables a configuration with less delay than that of retransmission control, we adopt FEC in this paper and refer to this configuration as the single path configuration with FEC.

In light of the above, in this paper, to determine the network configuration that satisfies the requirements, we examine the roundtrip-delay criteria. We also examine the area coverage of remote production in accordance with the actual environment that satisfies the roundtrip-delay requirement in the diverse path configuration with seamless switching and the single path configuration with FEC.

IV. ROUNDTRIP-DELAY REQUIREMENT TEST

In this section, we describe the experiment we performed to determine the roundtrip-delay requirement in remote production. The examination configuration is shown in Fig. 3. We compare the remote production system with the conventional production system which uses SDI only. The remote production system uses SDI and IP jointly. The video cameras were operated at 2K with a 59.94-Hz progressive frame (2K59p, 16.7 ms/frame) and at 2K with a 59.94-Hz interlace frame (2K59i, 33.4 ms/frame) to determine the effect of different frame resolutions. In both systems, two video sources were switched during the test: Video A, where the shot video was displayed in the viewfinder (VF) directly and Video B, where the return video was output from a camera control unit (CCU), a switched signal at the video switcher was returned to the CCU, and both were displayed in the VF. The switching delay that occurred when switching between Video A and Video B displayed in the VF was used as an observation target. Since we shot the waving action of a hand with the camera, when the switching delay was small, Videos A and B switched smoothly, but when the switching delay was large, they switch unnaturally as if the video frames were dropped. For this test, at least ten broadcast technicians carried out the switching between Video A and Video B by pushing the button connected to the CCU to determine whether the switching delay in the remote production system was comparable to that in the conventional production system. The tests were repeated until each technician was satisfied subjectively, and the consensus of all the technicians was confirmed to evaluate the switching delay. The test results were decided to be "acceptable" if the broadcast technicians felt that the switching delay could achieve almost the same performance as remote production and "NOT acceptable" if not. To change the switching delay, the delay from the CCU output to the CCU input was adjusted by changing the set value of the buffering quantity of the IP packet buffer built in the IP to the SDI unit.

The results are shown in Table 1. The delay values from the CCU output to the CCU input were measured as seen in the table. Test 1 is the minimum delay value that can be achieved in the remote production system. In the case of conventional production, the delay value from the CCU output to the CCU input is approximately 30 μs, and it is difficult to recognize the switching delay between the two videos [34]. Test cases 1 and 2 used a 2K59p video frame. For test case 1 the measured delay from the CCU output to the CCU input is 16.7 ms, and for test case 2 it is 33.4 ms. On the other hand, test cases 3 and 4 used a 2K59i video frame. For test case 3 the delay from the CCU output to the CCU input is 33.4 ms, and for test case 4 it is 66.8 ms. As we can see, the acceptable delay from the CCU output to the CCU input is either 16.7 ms or 33.4 ms. On the other hand, in test cases 3 and 4, which used the 2K59i video frame, a delay

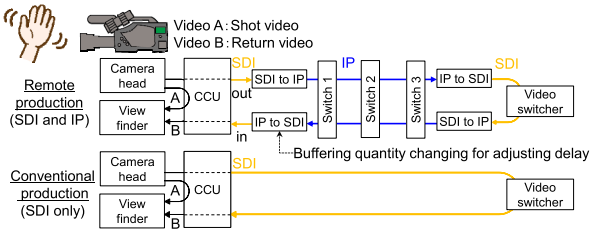

FIGURE 3. Examination configuration. We prepared two configurations, remote production and conventional production, and checked the switching delay between A: shot video and B: return video in each.

TABLE 1. Test results.

Test case	No. 1	No. 2	No. 3	No. 4
Video frame	59p (16.7 ms/frame)		59i (33.4 ms/frame)	
Delay from CCU out to CCU in (ms)	16.7	33.4	33.4	66.8
Test result	Acceptable	Acceptable	Acceptable	NOT acceptable

of 33.4 ms is acceptable, while a delay of 66.8 ms is NOT acceptable. That is, there is an excessive delay compared to conventional production in the case of a 66.8 ms delay. On the basis of these findings, we conclude that if the CCU output to CCU input delay is 33.4 ms, the same operation as conventional production is possible with both 2K59p and 2K59i frames. Therefore, we set 33.4 ms as a criterion for the roundtrip-delay requirement in the remote production system environment. Since the roundtrip delay is the two-way transmission delay between the venue and the broadcasting station, the criterion of the one-way transmission delay is 16.7 ms, which is half of the roundtrip delay. We set this value as the transmission-delay requirement. In the next section, we examine the transmission delay using this criterion.

V. EVALUATION OF NETWORK CONFIGURATION

A. CONFIGURATION

As shown in Fig. 4, the transmission delay d_{td}, which is defined in Eq. (1), is the time it takes a transmitter input at a venue to be output by a receiver at a broadcasting station. It consists of the sum of the network-induced delay d_{nw}^{path} ($path = 1$ or 2, which means path no. 1 or path no. 2), the transmitter-induced delay d_{tx}, and the receiver-induced delay d_{rx}.

$$d_{\mathrm{td}} = d_{\mathrm{tx}} + d_{\mathrm{nw}}^{path} + d_{\mathrm{rx}}. \tag{1}$$

The network is divided into an access part consisting of switches and a metro/core part consisting of routers. The d_{nw}^{path} can be expressed as:

$$\begin{aligned} d_{\mathrm{nw}}^{path} = {} & \sum_{m=1}^{M_{\mathrm{tx}}} s_m + \sum_{m=1}^{M_{\mathrm{tx}}-1} p_{\mathrm{acs}}^{m} + \sum_{n=1}^{N_{path}} r_n + l_{\mathrm{pcs}} \\ & + \sum_{n=1}^{N_{path}-1} p_{\mathrm{mtr}}^{n} + \sum_{m=1}^{M_{\mathrm{rx}}} s_m + \sum_{m=1}^{M_{\mathrm{rx}}-1} p_{\mathrm{acs}}^{m}, \end{aligned} \tag{2}$$

where M_{tx} is the number of switches on the transmitter side and M_{rx} is the number of switches on the receiver side. N_{path} is the number of routers belonging to path 1 or path 2. s_m ($m = 1, \ldots, M_{\mathrm{tx}}$ or $1, \ldots, M_{\mathrm{rx}}$) denotes the switch delay, and r_n ($n = 1, \ldots, N_{path}$) denotes the router delay. l_{pcs} denotes the server processing latency in the cloud. p_{acs}^{m} and p_{mtr}^{n} are the m-th access propagation delay between switches and the n-th metro/core propagation delay between routers, respectively. The relationship between the access propagation delay p_{acs} and the access path length L_{acs}, the metro/core propagation delay p_{mtr} and the metro/core path length L_{mtr}^{path} can be expressed by:

$$p_{\mathrm{acs}} = \sum_{m=1}^{M_{\mathrm{tx}}-1} p_{\mathrm{acs}}^{m} + \sum_{m=1}^{M_{\mathrm{rx}}-1} p_{\mathrm{acs}}^{m} = L_{\mathrm{acs}}/v_{\mathrm{path}}, \tag{3}$$

$$p_{\mathrm{mtr}}^{path} = \sum_{n=1}^{N_{path}-1} p_{\mathrm{mtr}}^{n} = L_{\mathrm{mtr}}^{path}/v_{\mathrm{path}}, \tag{4}$$

where v_{path} represents the propagation speed in fiber optics, which generally is considered to be 2.0×10^8 m/s. In this study, on the transmission route of the main line and subline, we assume the same route for the access part and a different route for the metro/core part.

The transmitter-induced and receiver-induced delays are varied depending on the transmission equipment configuration. In this paper, we examined the two transmission equipment configurations shown in Fig. 5(a) and (b). Fig. 5(a) shows a diverse path configuration with seamless switching (DPC) used for the transmission equipment. This configuration is available when redundant paths can be allocated. A buffer is also included for seamless switching between the main line and the subline when a problem occurs on the main line [37]. Fig. 5(b) shows a single path configuration with FEC processing (SPC) used for the transmission equipment. This configuration is available when redundant paths cannot be allocated, and FEC is applied as a technique for compensating for packet loss due to deterioration in transmission line quality. In both DPC and SPC, the use of video compression and decompression techniques results in processing delay. The transmitter-induced delay d_{tx} and the receiver-induced delay d_{rx} in Fig. 4 can be expressed by:

$$\begin{aligned} \text{for DPC;} \quad & d_{\mathrm{tx}} = c_{\mathrm{tx}}, \\ & d_{\mathrm{rx}} = b_{\mathrm{jit}} + b_{\mathrm{sml}} + c_{\mathrm{rx}}, \end{aligned} \tag{5}$$

$$\begin{aligned} \text{for SPC;} \quad & d_{\mathrm{tx}} = c_{\mathrm{tx}} + f_{\mathrm{tx}}, \\ & d_{\mathrm{rx}} = b_{\mathrm{jit}} + f_{\mathrm{rx}} + c_{\mathrm{rx}}, \end{aligned} \tag{6}$$

where c_{tx} and c_{rx} represent the processing delays required for compression and decompression, respectively, b_{jit} represents the buffer delay for absorbing packet jitter in a transmission path, and b_{sml} represents the seamless switching buffer delay when switching between the main line and the subline without interruption when a failure occurs. The delay difference of two lines in the receiver input is set to b_{sml} and switching without interruption is achieved by delaying the system with only a small delay. f_{tx} and f_{rx} represent delays related to the FEC encoding processing and decoding processing, respectively. The FEC we examined here is assumed to be a diagonal XOR-based FEC suitable for the transmission of 4K/8K high-speed video signals as described in the literature [35]. In this method, packets to be transmitted are virtually arranged in two dimensions, and XOR operations between packets in diagonal directions are performed. Compared to the conventional method of performing XOR operations between packets in the row and column directions [36], this method has an advantage in that the burst loss tolerance can be doubled while the random loss tolerance remains unchanged. The parameters and symbols used in this evaluation are summarized in Table 2.

B. NETWORK MODEL AND ROUTING SELECTION

We evaluated the transmission delay in a real-world network environment through simulations using four network models, which are listed in Table 3: the Japan Photonic Network (JPN) model [37], the GEANT model [38], the TW Telecom network (TTN) model [39], and the China Telecom Network (CTN) model [40]. Fig. 6 shows the JPN model, and

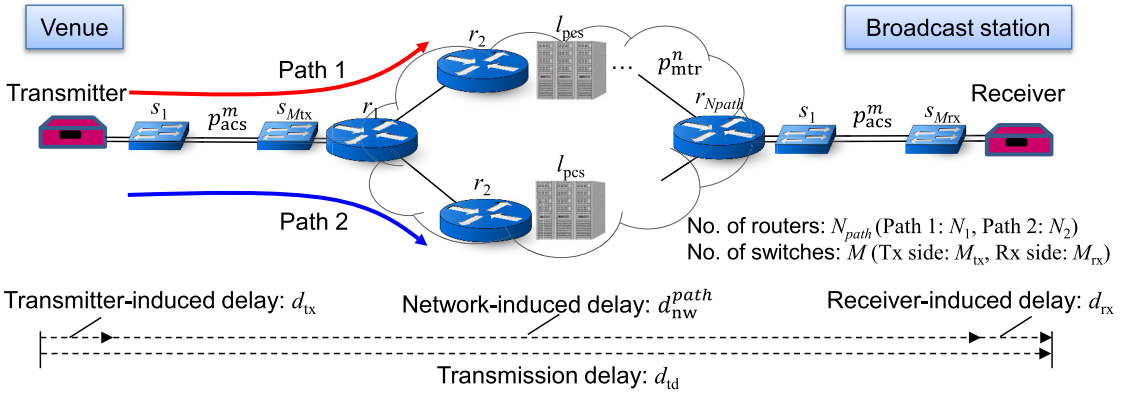

FIGURE 4. Network configuration used to study network requirements. Transmission delay is the time it takes a transmitter input at a venue to be output by a receiver at a broadcasting station. It consists of the sum of the transmitter-induced delay, the network-induced delay, and the receiver-induced delay.

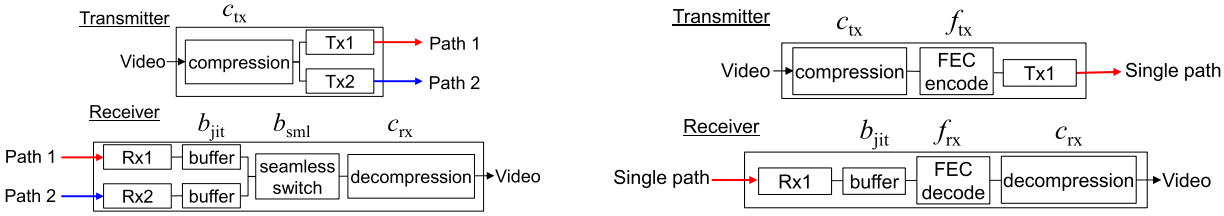

(a) Diverse paths configuration with seamless switching (DPC)

(b) Single path configuration with FEC processing (SPC)

FIGURE 5. Transmission equipment configurations used to study network requirements. DPC uses seamless switch between two paths to prevent video degradation. SPC uses FEC processing to a single path to reduce video quality degradation.

TABLE 2. List of parameters and symbols.

Parameter	Symbol
Transmission delay	d_{td}
Transmitter-induced delay	d_{tx}
Receiver-induced delay	d_{rx}
Network-induced delay	d_{nw}^{path}
Number of switches	M_{tx}, M_{rx}
Passing delay per switch	s_m
Access propagation delay	p_{acs}
Number of routers	N_{path}
Passing delay per router	r_n
Server processing latency	l_{pcs}
Metro/core propagation delay	p_{mtr}^{path}
Comp. and decomp. delay	c_{tx}, c_{rx}
Receiver buffer delay	b_{jit}
Seamless switch delay	b_{sml}
FEC processing delay	f_{tx}, f_{rx}
Access and metro/core path length	L_{acs},L_{mtr}^{path}
Propagation speed in fiber	v_{path}
Coverage rate	R_{cov}

TABLE 3. Network models.

Network model		JPN	GEANT	TTN	CTN
Region		Japan	Europe	USA	China
Network date		2016	2012	2010	2010
Number of nodes		48	37	70	38
Number of links		164	122	230	132
Degree	Average	3.42	3.30	3.29	3.47
	Max	6	11	12	20
Links length (km)	Average	153.8	909.0	533.1	919.5
	Max	758	3221.7	4155.4	2567.1
	Min	10	54.9	13.5	80.5
Node source city		Tokyo	Paris	Washington, D.C.	Beijing

Fig. 12 in the appendix shows the others. Each model discloses node information, including geographic information, and the distances between links connecting the nodes. Based on this information, we constructed a simulation environment using MATLAB. When examining the network configuration of remote production, using models that simulate the existing network environment is indispensable. In this section, we report the results of the JPN model as a representative example. The JPN model constructs a network that covers all of Japan on the basis of widely announced information such as that from railway networks. The JPN model is similar to the real networks used by major telecommunication companies in Japan, and we utilize it here to simulate the real environment. We used the JPN48 model (shown in Fig. 6), in which one information communication node is arranged in each prefecture and the nodes are interconnected by a flat network that is not hierarchized. Since only Tokyo has two information communication nodes (Tokyo and Hachioji), the number of information communication nodes is 48, which is the number of prefectures +1, and the transmission distance considering the geographical characteristics between each node is known.

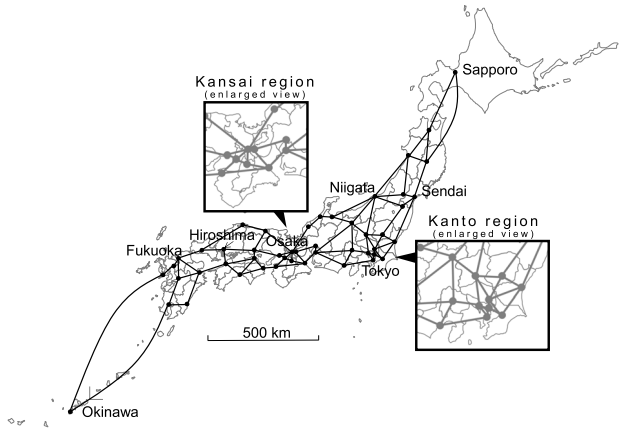

FIGURE 6. JPN48 model. At least one node is placed in each prefecture.

Routing selection algorithm

ns = Node_source, *nd* = Node_destination, *td* = Transmission_distance
for *i* = 1 to 47
  SRC = 'Tokyo', *DEST* = *ns*(*i*) except *SRC*
  /* Search for Path 1 (main-line) */
  G_1 = undirected_graph_generation(*ns*, *nd*, *td*)
  [Node_path_1, $L_{\mathrm{mtr}}^{path=1}$] = shortest_path_search(G_1, *SRC*, *DEST*)

  /* Search for Path 2 (subline) */
  [*ns*', *nd*'] = remove_path(*ns*, *nd*, Node_path_1)
  G_2 = undirected_graph_generation(*ns*', *nd*', *td*)
  [Node_path_2, $L_{\mathrm{mtr}}^{path=2}$] = shortest_path_search(G_2, *SRC*, *DEST*)
end for

FIGURE 7. Pseudocode for routing selections. The path where the shortest distance between the source and destination cities is calculated is set to Path 1, and the path where the shortest distance is calculated again after deleting links in Path 1 is set to Path 2.

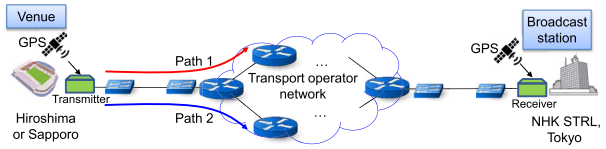

FIGURE 8. Average passing delay per router measurement configuration. A commercial line was used to measure the actual delay.

TABLE 4. Average passing delay per router.

Venue	Hiroshima		Sapporo	
Path	#1	#2	#1	#2
Measured delay (ms)	7.327	9.324	6.532	11.812
Number of routers	5	7	3	4
Number of switches	4	4	4	4
Metro/core path length on JPN (km)	894	1164	945	1885
Average passing delay per router (ms)	0.57	0.50	0.59	0.60

The pseudocode we used for routing selections is shown in Fig. 7. In route selections, generally speaking, the conditions under which the propagation delay reaches its minimum and the same transmission route does not pass twice are set. For our evaluation setup, we first created an undirected graph G_1 of 48 nodes with distance as the weight. We search for a route having the shortest distance in the case where any of the source and 47 nodes are set to the destination from G_1 and then set path 1 as the route to the main line. "Node_path_1" stores path 1's all selected nodes, and "$L_{\mathrm{mtr}}^{path=1}$" stores the metro/core path length for path 1. Next, paths applied to the path selection of path 1 are deleted from G_1, except for the case in which path 1's node has only one path, and an undirected graph G_2 is created from the remaining nodes. Similarly, a route having the shortest distance from G_2 is searched, and this is set as path 2 as the subline. "Node_path_2" stores path 2's all selected nodes, and "$L_{\mathrm{mtr}}^{path=2}$" stores the metro/core path length for path 2. With this route selection, for example, on the route between Tokyo as a source and Sendai as a destination, the main-line Tokyo - Omiya - Utsunomiya - Fukushima - Sendai ($L_{\mathrm{mtr}}^{path=1}$: 351.8 km) and the subline Tokyo - Chiba - Mito - Sendai ($L_{\mathrm{mtr}}^{path=2}$: 412.1 km) are selected. We perform route selections in the same way for the other three network models.

C. AVERAGE PASSING DELAY PER ROUTER

Routers located on the network are essential for signal routing. The number of passing routers varies depending on the transmission path. The network-induced delay increases as the number of passing routers increases. In addition, since the router multiplexes and processes various signals, the passing delay per router varies depending on the load state of the router. Therefore, we calculated an average passing delay per router based on the actual measurement. Fig. 8 shows the measurement configuration. For this measurement, we designated two locations, Hiroshima city and Sapporo city, as venues and connected each location to NHK STRL (located in Tokyo) via a commercial line to measure the network-induced delay from end to end. A commercially available measuring instrument was used for the network-induced delay measurement. To avoid sampling time errors, the measuring instruments of both the transmitter and receiver were locked by the global positioning system (GPS). The straight distance from the NHK STRL is approximately 670 km for Hiroshima city and 840 km for Sapporo city. Table 4 shows the measured results and the average passing delay per router calculated using the JPN model. The number of routers and switches that passed through the measurement were obtained by requesting information disclosure from the telecommunications carrier. In addition, the major transit nodes of paths 1 and 2 are disclosed, and the metro/core path length calculated from the JPN model based on this information is also shown. When the venue was Hiroshima city, path 1 had five routers, four switches, and a measured delay of 7.327 ms. The metro/core path length L_{mtr}^{path} on the JPN model was 894 km. In this case, the metro/core propagation delay p_{mtr}^{path} was calculated to be 4.47 ms by using Eq. (4). The passing delay per switch s_m had a very low latency of 0.001 ms [41], and the access path length was less than approximately five kilometers. Then, the access propagation delay p_{acs} was calculated as 0.025 ms by using Eq. (3), so we can calculate the average passing delay per router for Hiroshima city to be 0.57 ms. Similarly, path 2 was calculated to be 0.50 ms. When the venue was Sapporo city, the same procedure was used to calculate the average passing delay per router, for path 1 resulting in 0.59 ms and for path 2 in 0.60 ms. These results were calculated on the basis of actual measurements and thus are considered valid [42]. On the basis of these results, we set

TABLE 5. Simulation parameters.

Parameter			Value
Number of switches		M_{tx}, M_{rx}	2
Passing delay per switch		s_m	0.001 ms
Access propagation delay		p_{acs}	0.2 ms (L_{acs}: 40-km path length)
Number of routers		N_{path}	2–10 ($N_1 = N_2$)
Passing delay per router		r_n	Poisson dist. (average: 0.56 ms)
Server processing latency		l_{pcs}	2–10 ms
Metro/core propagation delay		p_{mtr}^{path}	Calc. from network model
Comp. and decomp. delay		c_{tx}, c_{rx}	0.3 ms
Receiver buffer delay		b_{jit}	2 ms
Seamless switch delay		b_{sml}	Calc. from network model
FEC processing delay	$X = 10$	$f_{\mathrm{tx}} + f_{\mathrm{rx}}$	0.312 ms
	$X = 20$		0.961 ms
Propagation speed of fiber		v_{path}	2.0×10^8 m/s

the average passing delay per router in the next section to 0.56 ms.

D. SIMULATION RESULTS

Table 5 summarizes the simulation parameters. In this evaluation, in the case of DPC, we assumed different routes for the metro/core part for the two transmission paths (path 1 and path 2). M_{tx} and M_{rx} were set to 2, and s_m was set to 0.001 ms when operating in cut-through mode with 10 GbE [41]. We assumed that switches are installed at both ends of the access line. A delay of 0.2 ms was set as p_{acs} assuming a total access line L_{acs} of 40 km on both the transmitting and receiving sides together. N_{path} was changed from 2 to 10. We set $N_1 = N_2$ for simplicity. r_n is the sum of the process delay, queuing delay, and serialization delay. The value of r_n was set to the Poisson distribution [27], and its average was 0.56 ms given the results obtained from field examinations (as described in the previous section and past research [23], [42]). l_{pcs} is the server processing latency in the cloud. $c_{\mathrm{tx}}$and c_{rx} were set to 0.3 ms apart, which is the measured value of our developed transceiver [19]. b_{jit} was set to 2 ms. The metro/core propagation delay p_{mtr}^{path} and the seamless switch buffer delay b_{sml} were calculated from each network model. p_{mtr}^{path} was calculated as the metro/core path length L_{mtr}^{path} between the Node_source and Node_destination of Path 1 or Path 2 calculated by the pseudocode in Fig. 7, divided by the propagation speed of fiber $v_{\mathrm{path}} = 2.0 \times 10^8$ m/s defined by Eq. (4). b_{sml} was calculated as $\left| p_{\mathrm{mtr}}^{path=1} - p_{\mathrm{mtr}}^{path=2} \right|$.

In the case of SPC, the path with the minimum calculated propagation delay was selected. An FEC block is defined as a group of X video packets and one FEC packet for error correction [35]. X represents the number of video packets in the FEC block. The value of X is related to the error correction capability. If X is increased, the number of video packets for one FEC packet in the FEC block increases, thus degrading the random packet loss correction performance while improving the burst packet loss correction performance. In this paper, X of SPC was examined at 10 and 20 packets. The random packet loss rate (PLR) after FEC processing can be expressed by:

$$PLR = \sum_{n=1}^{N} \left\{ \sum_{a=1}^{X-2} \frac{X-aC_2}{n} (1 - RLR)^{-(\mathrm{X-n})} \right\} RLR^n, \tag{7}$$

where RLR is the random packet loss rate before FEC processing with $RLR \leq 0.1$ generally, and N is the number of lost packets with $N \geq 4$. The PLR requires approximately 10^{-6} or less when the RLR is 10^{-3}, as indicated in appendix XI of [43]. The PLR at this time becomes 3.2×10^{-7} ($X = 10$) and 2.4×10^{-6} ($X = 20$). The packet loss period (LP) defines the maximum number of consecutive burst packets that can be lost, and in appendix VIII of [43], LP = 10 is indicated as an example. The recovery LP defines the maximum number of consecutive burst packets that can be completely recovered, and in a proposed FEC processing method [35], the recovery LP can be expressed by:

$$recovery\ LP \leq 2X. \tag{8}$$

The recovery LP becomes 20 ($X = 10$) and 40 ($X = 20$). In this method, the FEC processing delay $f_{\mathrm{tx}} + f_{\mathrm{rx}}$ becomes 0.312 ms ($X = 10$) and 0.961 ms ($X = 20$) [35].

Fig. 9 shows a deterministic metro/core path length L_{mtr} when d_{td} is fixed to 16.7 ms. L_{mtr} can be calculated by:

$$L_{\mathrm{mtr}} = v_{\mathrm{path}} \{16.7 - d_{\mathrm{tx}} - d_{\mathrm{rx}} - \left(\sum_{m=1}^{M_{\mathrm{tx}}} s_m + \sum_{n=1}^{N_{path}} r_n + l_{\mathrm{pcs}} + \sum_{m=1}^{M_{\mathrm{rx}}} s_m + p_{\mathrm{acs}} \right) \}. \tag{9}$$

Fig. 9(a)–(c) shows the results of DPC, SPC ($X = 10$), and SPC ($X = 20$), respectively. As an example of a specific calculation, when N_{path} is 0 and l_{pcs} is 2 ms in Fig. 9(a), L_{mtr} can be calculated by $\{2.0 \times 10^8 \times (16.7 - 0.3 - 4.3 - 2.204) \times 10^{-3}\}$ and then reaches approximately 1,980 km. We can see that SPC ($X = 10$) has the longest path length. In a real environment, since the transmission delay d_{td} of each path varies depending on the value of r_n stochastically, we define d_{td} as the value where the cumulative distribution function exceeds 99.9% for calculating the transmission delay 10^4 times for each path in the simulation. Fig. 10 shows representative simulation results of the transmission delay d_{td} calculated on the basis of the requirements for each node (all nodes) on the JPN network model, where (a)–(c) show the results of DPC, SPC ($X = 10$), and SPC ($X = 20$), respectively. The number of routers N_{path} is set to 4, and the server processing latency in the cloud l_{pcs} is set to 6 ms. The white color in Fig. 10 represents a transmission delay d_{td} of 16.7 ms, red a d_{td} of less than 16.7 ms, and blue represents a d_{td} value greater than 16.7 ms. In other words, the white-to-red color area can satisfy the transmission-delay requirement, and the darker the red color is, the more margin d_{td} has for the transmission-delay requirement. To improve visibility, we color the entire node where the transmission-delay requirement is satisfied but note that the transmission-delay requirement is satisfied within a fiber length range of 20 km

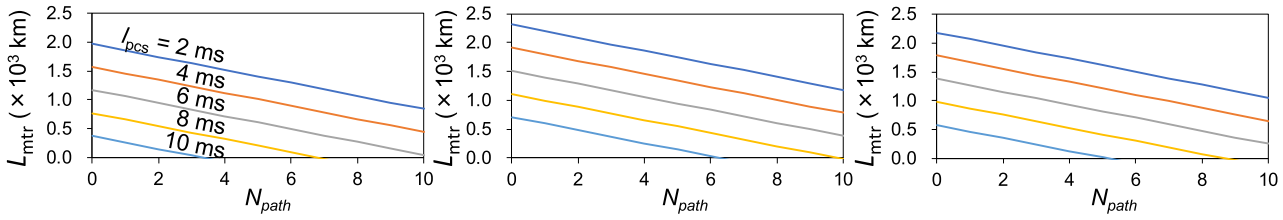

(a) DPC (b_{sml} = 2 ms) (b) SPC (X = 10) (c) SPC (X = 20)

FIGURE 9. Theoretical value of deterministic metro/core path length L_{mtr} to fix transmission delay d_{td} of 16.7 ms for DPC, SPC (X = 10), and SPC (X = 20).

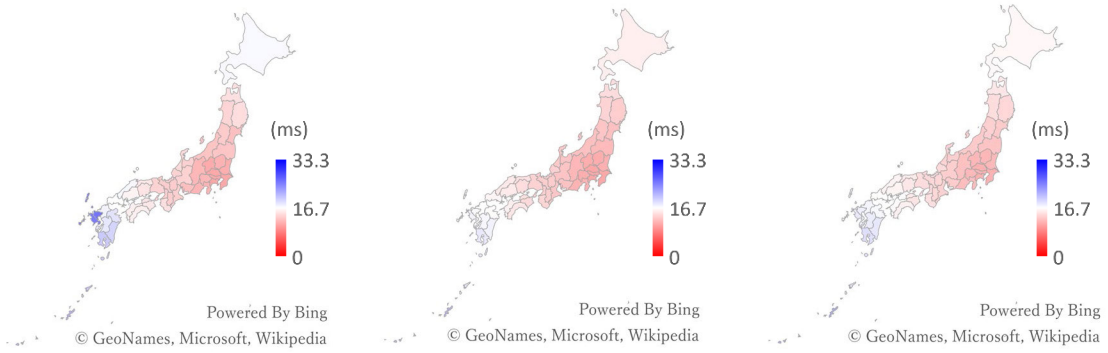

(a) DPC (b) SPC (X = 10) (c) SPC (X = 20)

FIGURE 10. Example simulation results of d_{td} in the JPN model for DPC, SPC (X = 10), and SPC (X = 20). N_{path} = 4 and l_{pcs} = 6 ms.

TABLE 6. Example simulation results of d_{td} in each model.

(a) JPN

Venue	DPC (ms)	SPC (X = 10) (ms)	SPC (X = 20) (ms)	Length (km) Path 1	Length (km) Path 2
Yokohama	11.0	11.0	11.6	28.8	83.9
Nagoya	12.6	12.7	13.4	366.0	396.9
Osaka	13.6	13.6	14.2	552.6	604.9
Kobe	13.9	13.8	14.4	589.5	672.0
Sapporo	17.1	15.6	16.2	945.1	1303.8

(b) GEANT

Venue	DPC (ms)	SPC (X = 10) (ms)	SPC (X = 20) (ms)	Length (km) Path 1	Length (km) Path 2
London	16.5	12.7	13.3	344.2	1201.1
Frankfurt	14.5	13.2	13.9	479.1	799.8
Milano	19.1	14.1	14.7	648.3	1703.6
Madrid	18.5	16.1	16.8	1053.6	1588.7
Moscow	25.0	23.3	24.0	2501.9	2885.4

(c) TTN

Venue	DPC (ms)	SPC (X = 10) (ms)	SPC (X = 20) (ms)	Length (km) Path 1	Length (km) Path 2
New York	17.0	12.5	13.2	328.9	1293.4
Chicago	15.9	15.6	16.3	957.5	1060.5
Houston	21.5	21.0	21.6	2020.9	2184.3
Phoenix	28.6	28.1	28.8	3450.5	3617.7
Los Angeles	32.3	30.9	31.6	4021.8	4348.7

(d) CTN

Venue	DPC (ms)	SPC (X = 10) (ms)	SPC (X = 20) (ms)	Length (km) Path 1	Length (km) Path 2
Wuhan	20.2	16.1	16.8	1055.9	1358.6
Shanghai	15.9	16.2	16.8	1069.5	1071.9
Hangzhou	16.7	17.0	17.7	1233.2	1235.6
Guangzhou	20.2	20.3	21.0	1892.5	1930.6
Chongqing	24.9	23.7	24.4	2574.1	2872.5

from each node position. As we can see in the figure, the number of red areas shown for SPC is higher than that of DPC. For example, when comparing Sapporo city, the northernmost city on the map, DPC shows a blue area, while SPC is closer to the red area in the case of both $X = 10$ and $X = 20$. This indicates that SPC can reduce the value of d_{td} more than DPC. Table 6 shows the results of calculating d_{td} for each network model. In this table, the number of routers N_{path} is set to 4, and the server processing latency in the cloud l_{pcs} is set to 6 ms, as shown in Fig. 10. We also applied the same color based on 16.7 ms. The values shown in Fig. 10 correspond to those shown for Sapporo city in Table 6(a). In the table, the five cities with the highest population among the nodes in each network model are listed in ascending order based on the length of path 1. In the case of the JPN model in Table 6(a), the path length is relatively short compared to the other network models, so the transmission-delay requirement is generally satisfied for the major cities. On the other hand, for Sapporo city, the path length of the redundant paths of path 2 for DPC is 1303.8 km, which is longer than those of the other cities, and the path length difference between paths 1 and 2 is 360 km, which is large, resulting in a d_{td} of 17.1 ms, which does not meet the transmission-delay requirement. In the other network models, the distance between nodes tends to be longer, so fewer nodes are able to meet the transmission-delay requirement. In all tables, we can see that

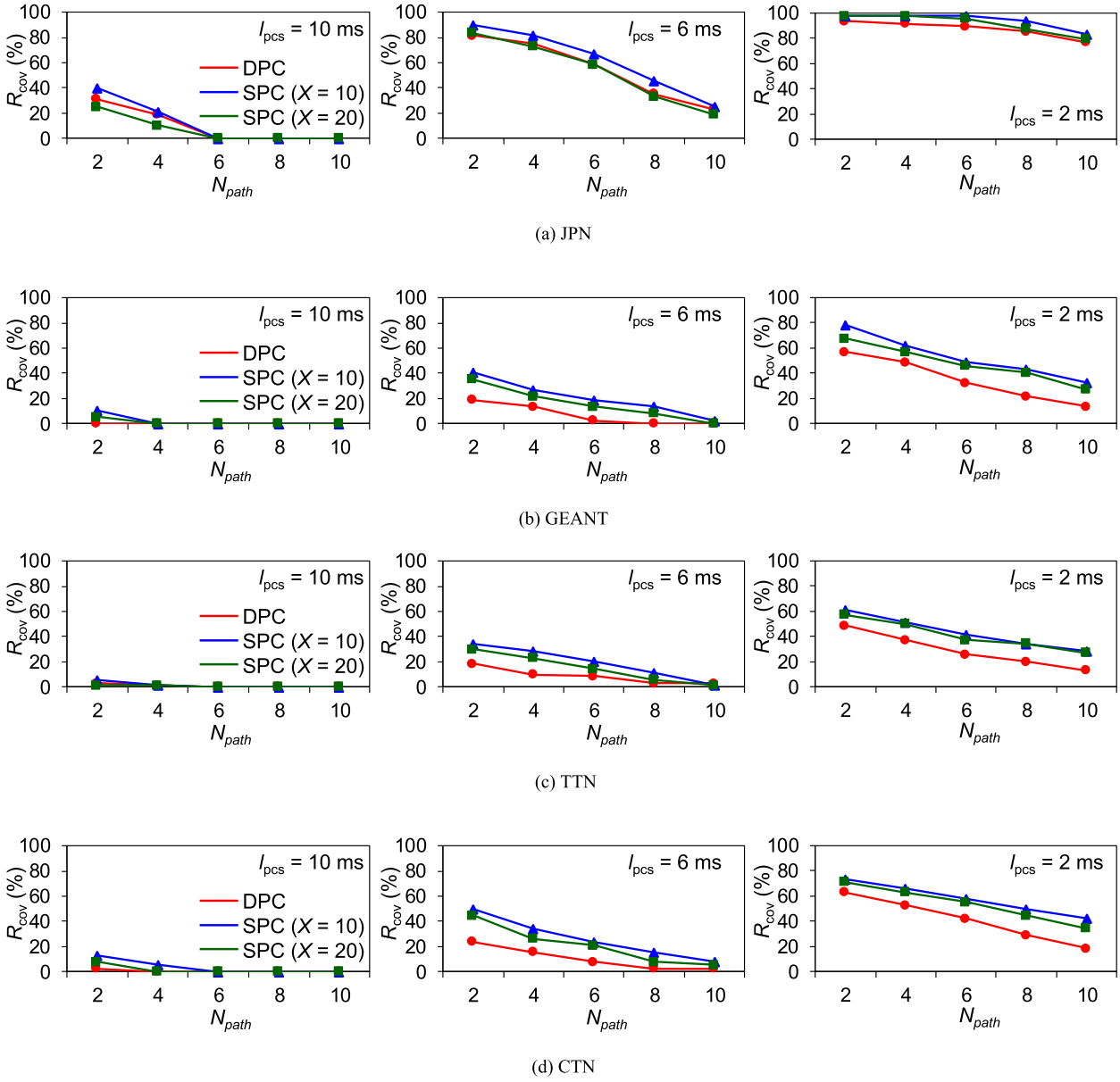

FIGURE 11. R_{cov} versus N_{path} in each model for DPC, SPC ($X = 10$), and SPC ($X = 20$).

the path length of DPC depends on the path length of path 2 and the path length difference between paths 1 and 2. On the other hand, for SPC ($X = 10$), the transmission-delay requirement of 16.7 ms or less can be achieved if the path length of path 1 is approximately 1050 km or less, and for SPC ($X = 20$), a path length of 950 km or less can be achieved, which is even shorter than that in Fig. 9. From the viewpoint of network design, DPC requires consideration of not only the path length but also the path length difference, while SPC has the advantage of relatively simple design work because the transmission delay d_{td} is determined by setting one path.

Next, we investigate how much area coverage can be achieved for each method in each network model, considering the server processing latency in the cloud. Fig. 11 shows the coverage rate R_{cov} with respect to the number N_{path} of routers when l_{pcs} is changed with the destination node as the source point. The coverage rate R_{cov} is shown in each figure. R_{cov} defines "the number of nodes below the estimated transmission-delay requirement for all nodes in the network model" as a percentage. Fig. 11(a)–(d) shows the results of the JPN model, GEANT model, TTN model, and CTN model, respectively. In each figure, l_{pcs} is equal to 10 ms, 6 ms, or 2 ms. As shown in Fig. 11(a), when l_{pcs} is 10 ms, R_{cov} is zero if N_{path} is greater than or equal to 6. This means that there is no node that can satisfy $d_{td} = 16.7$ ms. On the other hand, when l_{pcs} becomes as low as 6 ms, R_{cov} becomes approximately 50% when N_{path} is 6, and the transmission-delay requirement can be satisfied at half of the nodes in the JPN model. Furthermore, when l_{pcs} is 2 ms,

(a) GEANT

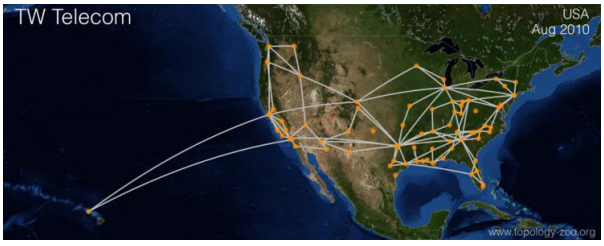

(b) TTN

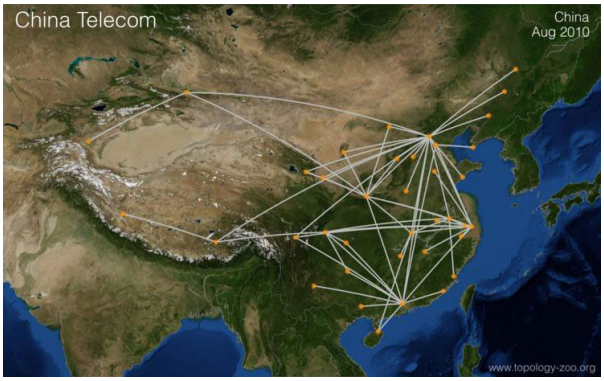

(c) CTN

FIGURE 12. **Topology of each network model.**

R_{cov} improves significantly, and even when N_{path} is 10, R_{cov} is approximately 80%, which satisfies the transmission-delay requirement for almost all nodes. In the network models of GEANT and TTN (Fig. 11(b) and (c)), an l_{pcs} of 2 ms is required to achieve an R_{cov} of approximately 50% for DPC and SPC. On the other hand, in the network model of CTN (Fig. 11(d)), in the case of SPC ($X = 10$), an R_{cov} of 50% can be achieved when N_{path} is 2 even if l_{pcs} is 6 ms. In each configuration, we find that the server processing latency in the cloud should be kept in the range of 2–6 ms to satisfy the transmission-delay requirement.

In all cases of Fig. 11(a)–(d), R_{cov} can be increased in the order of SPC ($X = 10$), SPC ($X = 20$), and DPC. When l_{pcs} is 2 ms and N_{path} is 6, the improvement rate of SPC ($X = 10$) over DPC is 1.42 times for the GEANT model, 1.44 times for the TTN model, and 1.31 times for the CTN model, compared to just 1.07 times for the JPN model. The reason the improvement rates of the other network models are higher than that of the JPN model is that DPC's R_{cov} values used for calculating the improvement rates are lower than those of the JPN model. The JPN model has a relatively short route length; therefore, it can achieve a sufficient coverage rate even with DPC.

These results demonstrate the importance of setting the server processing latency l_{pcs} when designing a network configuration of remote production in a way that satisfies the required transmission delay. We also found that the FEC configuration based on SPC could improve the coverage rate satisfying the transmission-delay requirement more than that based on DPC.

VI. CONCLUSION

In this paper, we investigated the roundtrip-delay requirement for a remote professional media production system. Then, we utilized the results to determine which network configuration enables remote production on the JPN, GEANT, TTN, and CTN models.

Our findings showed that if the delay from the CCU output to the CCU input (via the broadcast video switcher) of the venue's camera was 33.4 ms, the same operation as the conventional production work style using SDI was possible. This value was set as a criterion of the roundtrip-delay requirement in a remote production environment using SDI and IP jointly. Since the roundtrip delay was the two-way transmission delay between the venue and the broadcasting station, the standard of the one-way transmission delay was 16.7 ms, which is half of the roundtrip delay requirement.

On the basis of these values, we next investigated how much area coverage could be achieved while satisfying the transmission-delay requirement in each network model, considering the server processing latency l_{pcs} in the cloud. In the JPN model, when l_{pcs} became as small as 6 ms, the coverage rate R_{cov} became approximately 50% when N_{path} was 6. Furthermore, when l_{pcs} was 2 ms, R_{cov} improved significantly, and even when N_{path} was 10, R_{cov} was approximately 80%, which satisfied the transmission-delay requirement for almost all nodes. In the network models of GEANT and TTN, an l_{pcs} of 2 ms was required to achieve an R_{cov} of approximately 50% for DPC and SPC. On the other hand, in the network model of CTN, in the case of SPC ($X = 10$), an R_{cov} of 50% could be achieved when N_{path} was 2 even if l_{pcs} was 6 ms. In each configuration, we found that the server processing latency in the cloud should be kept in the range of 2–6 ms to satisfy the transmission-delay requirement. We also found that R_{cov} could be increased in the order of SPC ($X = 10$), SPC ($X = 20$), and DPC. When l_{pcs} was 2 ms and N_{path} was 6, the improvement rate of

SPC ($X = 10$) over DPC was 1.42 times for the GEANT model, 1.44 times for the TTN model, and 1.31 times for the CTN model, compared to only 1.07 times for the JPN model. These results should be useful for helping broadcasters design future remote production systems using a low-latency cloud network.

APPENDIX

The topology of each network model is shown in Fig. 12. Fig. 12(a) shows the GEANT network model in Europe, Fig. 12(b) shows the TTN network model in the USA, and Fig. 12(c) shows the CTN network model in China. In each figure, information communication nodes and the links connecting them are shown. The information about each network model is found in Table 3.

REFERENCES

[1] *Professional Media Over Managed IP Networks: System Timing and Definitions*, document SMPTE ST 2110-10:2017, 2017.
[2] S. Sneddon, C. Swisher, and J. Mayzurk, "Engineering design challenges in realization of a very large IP-based television facility," *SMPTE Motion Imag. J.*, vol. 129, no. 4, pp. 1–9, 2020.
[3] F. Poulin, P. Keroulas, S. Nyamweno, W. Vermost, P. Ferreira, and I. Kostiukevy, "How CBC/radio-Canada tested media-over-IP devices to build its new facility," *SMPTE Motion Imag. J.*, vol. 129, no. 4, pp. 35–44, 2020.
[4] H. Gaggioni, M. Ueda, F. Saga, K. Tomita, and N. Kobayashi, "Serial digital interface for HDTV," *SMPTE J.*, vol. 106, no. 5, pp. 298–304, May 1997.
[5] *IEEE Standard for Ethernet*, IEEE Standard 802.3, 2018.
[6] W. Na and X. Pin, "Cloud computing and its application in television and broadcasting industry," in *Proc. IEEE Int. Conf. Comput. Sci. Autom. Eng.*, Jun. 2012, pp. 372–375.
[7] R. Cartwright, "An Internet of Things architecture for cloud-fit professional media workflow," in *Proc. SMPTE Annu. Tech. Conf. Exhib.*, Oct. 2017, pp. 1–21.
[8] T. Witkowski and R. Welsh, "Media cloud fundamentals," *SMPTE Motion Imag. J.*, vol. 128, no. 9, pp. 26–33, 2019.
[9] D. Luzuriaga, C.-H. Lung, and M. Funmilayo, "Software-based video–audio production mixer via an IP network," *IEEE Access*, vol. 8, pp. 11456–11468, 2020.
[10] B. Johnston, "Taking remote production to the next level: CBC's coverage of the 2014 Sochi Olympic games," *SMPTE Motion Imag. J.*, vol. 124, no. 2, pp. 1–12, Mar. 2015.
[11] F. C. Chua, J. Ward, Y. Zhang, P. Sharma, and B. A. Huberman, "Stringer: Balancing latency and resource usage in service function chain provisioning," *IEEE Internet Comput.*, vol. 20, no. 6, pp. 22–31, Nov./Dec. 2016.
[12] J. Zhao, R. S. Allison, M. Vinnikov, and S. Jennings, "Estimating the motion-to-photon latency in head mounted displays," in *Proc. IEEE Virtual Reality*, Mar. 2017, pp. 313–314.
[13] T. Aykut, C. Zou, J. Xu, D. Van Opdenbosch, and E. Steinbach, "A delay compensation approach for pan-tilt-unit-based stereoscopic 360 degree telepresence systems using head motion prediction," in *Proc. IEEE Int. Conf. Robot. Autom. (ICRA)*, May 2018, pp. 3323–3330.
[14] M. Kountouris, P. Popovski, I.-H. Hou, S. Buzzi, A. Muller, S. Sesia, and R. W. Heath, Jr., "Guest editorial ultra-reliable low-latency communications in wireless networks," *IEEE J. Sel. Areas Commun.*, vol. 37, no. 4, pp. 701–704, Apr. 2019.
[15] H. S. Varsha and K. P. Shashikala, "The tactile internet," in *Proc. Int. Conf. Innov. Mech. Ind. Appl.*, 2017, pp. 419–422.
[16] Z. Xiang, F. Gabriel, E. Urbano, G. T. Nguyen, M. Reisslein, and F. H. P. Fitzek, "Reducing latency in virtual machines: Enabling tactile internet for human-machine co-working," *IEEE J. Sel. Areas Commun.*, vol. 37, no. 5, pp. 1098–1116, May 2019.
[17] M. Maier, M. Chowdhury, B. P. Rimal, and D. P. Van, "The tactile internet: Vision, recent progress, and open challenges," *IEEE Commun. Mag.*, vol. 54, no. 5, pp. 138–145, May 2016.
[18] K. S. Kim, D. K. Kim, C.-B. Chae, S. Choi, Y.-C. Ko, J. Kim, Y.-G. Lim, M. Yang, S. Kim, B. Lim, K. Lee, and K. L. Ryu, "Ultrareliable and low-latency communication techniques for tactile internet services," *Proc. IEEE*, vol. 107, no. 2, pp. 376–393, Feb. 2019.
[19] J. Kawamoto, T. Koyama, M. Kawaragi, K. Saito, and T. Kurakake, "Development of lightweight compressed 8K UHDTV over IP transmission device realizing live remote production," *ITE Trans. Media Technol. Appl.*, vol. 8, no. 1, pp. 31–39, 2020.
[20] *JPEG White Paper*. Accessed: May 20, 2021. [Online]. Available: http://ds.jpeg.org/whitepapers/jpeg-xs-whitepaper.pdf
[21] E. Calverley, "Time-compensated remote production over IP," *SMPTE Motion Imag. J.*, vol. 127, no. 5, pp. 51–57, Jun. 2018.
[22] M. Keltsch, S. Prokesch, O. P. Gordo, J. Serrano, T. K. Phan, and I. Fritzsch, "Remote production and mobile contribution over 5G networks: Scenarios, requirements and approaches for broadcast quality media streaming," in *Proc. IEEE Int. Symp. Broadband Multimedia Syst. Broadcast. (BMSB)*, Jun. 2018, pp. 1–7.
[23] J. Kawamoto, T. Koyama, M. Kawaragi, R. Shirato, T. Kurakake, and K. Saito, "Study of transmission-delay time for IP remote production of 8K UHDTV," in *Proc. IEEE Int. Symp. Local Metrop. Area Netw. (LANMAN)*, Jul. 2019, pp. 1–2.
[24] V. Petrov, M. A. Lema, M. Gapeyenko, K. Antonakoglou, D. Moltchanov, F. Sardis, A. Samuylov, S. Andreev, Y. Koucheryavy, and M. Dohler, "Achieving end-to-end reliability of mission-critical traffic in softwarized 5G networks," *IEEE J. Sel. Areas Commun.*, vol. 36, no. 3, pp. 485–501, Mar. 2018.
[25] Q. Ye, W. Zhuang, X. Li, and J. Rao, "End-to-end delay modeling for embedded VNF chains in 5G core networks," *IEEE Internet Things J.*, vol. 6, no. 1, pp. 692–704, Feb. 2018.
[26] K. Wang and H. Gu, "Understanding and modeling of the real application traffic characteristics for fast on-chip network evaluation," in *Proc. IEEE 18th Int. Conf. Commun. Technol. (ICCT)*, Oct. 2018, pp. 237–241.
[27] S. Choi, K. Shin, and H. Kim, "End-to-end latency prediction for general-topology cut-through switching networks," *IEEE Access*, vol. 8, pp. 13806–13820, 2020.
[28] *Arista Networks Homepage*. Accessed: May 20, 2021. [Online]. Available: https://www.arista.com/assets/data/pdf/CloudNetworkLatency.pdf
[29] T. H. Szymanski, "An ultra-low-latency guaranteed-rate internet for cloud services," *IEEE/ACM Trans. Netw.*, vol. 24, no. 1, pp. 123–136, Feb. 2016.
[30] H. Mei, K. Wang, and K. Yang, "Multi-layer cloud-RAN with cooperative resource allocations for low-latency computing and communication services," *IEEE Access*, vol. 5, pp. 19023–19032, 2017.
[31] D. Gehberger, D. Balla, M. Maliosz, and C. Simon, "Performance evaluation of low latency communication alternatives in a containerized cloud environment," in *Proc. IEEE 11th Int. Conf. Cloud Comput. (CLOUD)*, Jul. 2018, pp. 9–16.
[32] A. Khalek, C. Caramanis, and R. W. Heath, Jr., "Delay-constrained video transmission: Quality-driven resource allocation and scheduling," *IEEE J. Sel. Topics Signal Process.*, vol. 9, no. 1, pp. 60–75, Jan. 2015.
[33] *Seamless Protection Switching of RTP Datagrams*, document SMPTE ST 2022-7:2019, 2019.
[34] *MIT News*. Accessed: May 20, 2021. [Online]. Available: https://news.mit.edu/2014/in-the-blink-of-an-eye-0116
[35] J. Kawamoto and T. Kurakake, "Diagonal XOR-based FEC method to improve burst-loss tolerance for 4K/8K UHDTV transmission," *IEEE Trans. Circuits Syst. Video Technol.*, vol. 31, no. 5, pp. 1983–1994, May 2021.
[36] *Forward Error Correction for High Bit Rate Media Transport Over IP Networks*, document SMPTE ST 2022-5:2012, 2012.
[37] *Japan Photonic Network Model*. Accessed: May 20, 2021. [Online]. Available: https://www.ieice.org/cs/pn/jpn/jpnm.html
[38] *GÉANT Association Homepage*. Accessed: May 20, 2021. [Online]. Available: https://www.geant.org/
[39] *TW Telecom Dataset*. Accessed: May 20, 2021. [Online]. Available: http://www.topology-zoo.org/dataset.html
[40] *China Telecom Dataset*. Accessed: May 20, 2021. [Online]. Available: http://www.topology-zoo.org/dataset.html
[41] J. Woods, *Cut-Through Considerations and Impacts to Industrial Networks*, document IEEE 802.1 WG Interim Meeting, May 2017.
[42] T. Oishi, M. Takase, K. Sakamoto, and H. Endo, "Implementation of packet transport system using MPLS-TP technologies," in *Proc. 8th Asia–Pacific Symp. Inf. Telecommun. Technol.*, 2010, pp. 1–6.
[43] *Network Performance Objectives for IP-Based Services*, document ITU-T Y.1541, 2011.

JUNICHIRO KAWAMOTO received the M.E. and Ph.D. degrees from the University of Tsukuba, Ibaraki, Japan, in 2002 and 2017, respectively. From 2002 to 2008, he worked with the Research and Development Division, NTT DOCOMO, Inc. In 2008, he joined Japan Broadcasting Corporation (NHK). He has mainly been engaged in the research and development of professional media program production systems using IP-networks.

RYO SHIRATO received the B.E. and M.E. degrees from Waseda University, Tokyo, Japan, in 2014 and 2016, respectively. He joined Japan Broadcasting Corporation (NHK), in 2016. He has mainly been engaged in the research and development of 4K/8K UHDTV program production system using IP-networks.

TSUYOSHI NAKATOGAWA (Member, IEEE) received the B.E. and M.E. degrees in electrical and computer engineering from Yokohama National University, Kanagawa, Japan, in 1998 and 2000, respectively. He joined Japan Broadcasting Corporation (NHK), in 2000. Since 2003, he has been working with NHK STRL. He is currently a Senior Research Engineer with the Advanced Transmission Systems Research Division, where he is engaged in the development of next-generation terrestrial broadcasting systems for UHDTV and professional media program production systems using IP networks.

TAKUYA KURAKAKE received the B.E. and M.E. degrees from The University of Tokyo, Tokyo, Japan, in 1992 and 1994, respectively, and the Ph.D. degree from The University of Electro-Communications, Tokyo, in 2014. He joined Japan Broadcasting Corporation (NHK), in 1994. He has mainly been engaged in the research and development of an optical transmission system for cable television and digital cable television and a 4K/8K UHDTV program production system using IP networks. He received the Ichimura Prize in science, in 2005, and the Best Paper of the IEEE International Conference on Consumer Electronics (ICCE), in 2013.